JGR Atmospheres

RESEARCH ARTICLE
10.1029/2018JD029516

Large Impacts, Past and Future, of Ozone-Depleting Substances on Brewer-Dobson Circulation Trends: A Multimodel Assessment

L. M. Polvani[1,2,3], L. Wang[2,4], M. Abalos[5], N. Butchart[6], M. P. Chipperfield[7], M. Dameris[8], M. Deushi[9], S. S. Dhomse[7], P. Jöckel[8], D. Kinnison[3], M. Michou[10], O. Morgenstern[11], L. D. Oman[12], D. A. Plummer[13], and K. A. Stone[14,15,16]

[1]Department of Applied Physics and Applied Mathematics, Columbia University, New York, NY, USA, [2]Lamont-Doherty Earth Observatory, Columbia University, Palisades, NY, USA, [3]National Center for Atmospheric Research, Boulder, CO, USA, [4]Department of Atmospheric and Oceanic Sciences & Institute of Atmospheric Sciences, Fudan University, Shanghai, China, [5]Earth Physics and Astrophysics Department, Universidad Complutense de Madrid, Madrid, Spain, [6]Met Office Hadley Centre, Exeter, UK, [7]School of Earth and Environment, University of Leeds, Leeds, UK, [8]Deutsches Zentrum für Luft- und Raumfahrt, Oberpfaffenhofen, Germany, [9]Meteorological Research Institute, Tsukuba, Japan, [10]Météo-France/CNRS, Toulouse, France, [11]National Institute of Water and Atmospheric Research, Wellington, New Zealand, [12]NASA Goddard Space Flight Center, Greenbelt, MD, USA, [13]Climate Research Branch, Environment and Climate Change Canada, Montreal, Quebec, Canada, [14]School of Earth Sciences, University of Melbourne, Melbourne, Victoria, Australia, [15]ARC Centre of Excellence in Climate Science, University of New South Wales, Sydney, New South Wales, Australia, [16]Now at Department of Earth, Atmospheric, and Planetary Sciences, MIT, Cambridge, MA, USA

Abstract Substantial increases in the atmospheric concentration of well-mixed greenhouse gases (notably CO_2), such as those projected to occur by the end of the 21st century under large radiative forcing scenarios, have long been known to cause an acceleration of the Brewer-Dobson circulation (BDC) in climate models. More recently, however, several single-model studies have proposed that ozone-depleting substances might also be important drivers of BDC trends. As these studies were conducted with different forcings over different periods, it is difficult to combine them to obtain a robust quantitative picture of the relative importance of ozone-depleting substances as drivers of BDC trends. To this end, we here analyze—over identical past and future periods—the output from 20 similarly forced models, gathered from two recent chemistry-climate modeling intercomparison projects. Our multimodel analysis reveals that ozone-depleting substances are responsible for more than half of the modeled BDC trends in the two decades 1980–2000. We also find that, as a consequence of the Montreal Protocol, decreasing concentrations of ozone-depleting substances in coming decades will strongly decelerate the BDC until the year 2080, reducing the age-of-air trends by more than half, and will thus substantially mitigate the impact of increasing CO_2. As ozone-depleting substances impact BDC trends, primarily, via the depletion/recovery of stratospheric ozone over the South Pole, they impart seasonal and hemispheric asymmetries to the trends which may offer opportunities for detection in coming decades.

Key Points:
- Impacts of ozone-depleting substances (ODS) on Brewer-Dobson circulation trends are analyzed in 20 chemistry-climate models
- For the period 1980–2000 ODS have contributed more than half (roughly 60%) of the stratospheric age-of-air trends
- For the period 2000–2080 models show that decreasing ODS levels will substantially decelerate the BDC

Correspondence to:
L. Wang,
wanglei_ias@fudan.edu.cn

Citation:
Polvani, L. M., Wang, L., Abalos, M., Butchart, N., Chipperfield, M. P., Dameris, M., et al. (2019). Large impacts, past and future, of ozone-depleting substances on Brewer-Dobson circulation trends: A multimodel assessment. *Journal of Geophysical Research: Atmospheres*, *124*, 6669–6680. https://doi.org/10.1029/2018JD029516

Received 19 AUG 2018
Accepted 8 MAY 2019
Accepted article online 30 MAY 2019
Published online 2 JUL 2019

Author Contributions

Conceptualization: L. M. Polvani
Data curation: N. Butchart, M. P. Chipperfield, M. Dameris, S. S. Dhomse, P. Jöckel, D. Kinnison, M. Michou, O. Morgenstern, L. D. Oman, D. A. Plummer, K. A. Stone
Methodology: L. M. Polvani
Validation: M. Abalos
Writing - Original Draft: L. M. Polvani
Project Administration: L. M. Polvani
Writing - review & editing: M. Abalos, N. Butchart, M. P. Chipperfield, M. Dameris, S. S. Dhomse, P. Jöckel, D. Kinnison, M. Michou, O. Morgenstern, L. D. Oman, D. A. Plummer, K. A. Stone

1. Introduction

The meridional circulation in the stratosphere, known as the Brewer-Dobson circulation (hereafter BDC; Brewer, 1949; Dobson et al., 1929), is fundamental to our understanding of the distribution of ozone and other trace gases in the middle atmosphere, as well as their exchange across the tropopause. Documenting past and future BDC trends, and attributing such trends to specific anthropogenic emissions, is thus an integral part to understanding man-made climate change.

Although BDC trends over the last several decades have proven difficult to establish from observations (see Chapter 4 of WMO, 2014, for a recent review), it has long been known from modeling studies (e.g., Butchart & Scaife, 2001; Garcia & Randel, 2008; Rind et al., 1990) that increasing concentrations of well-mixed greenhouse gases (GHG), primarily CO_2, cause an acceleration of the BDC. This result is very robust, as it has been validated across dozens of models in several model intercomparison projects (Butchart et al., 2006, 2010; Hardiman et al., 2014). However, that result was largely established by contrasting the BDC in the late 20th and late 21st centuries, over which period CO_2 concentrations increase monotonically and roughly double

(for the modeling scenarios analyzed in most BDC trend studies). Over the satellite era (1979 to present), however, CO_2 concentrations have increased by much smaller amounts (a little over 20%) allowing for other anthropogenic emissions to play an important role.

Halogenated ozone-depleting substances (ODS), in particular, have been highlighted in a number of recent studies as being potentially important drivers of BDC trends. On the observational side, analyzing temperature trends from the microwave sounding units, Fu et al. (2015) uncovered a major hemispheric asymmetry in the dynamically driven cooling of the lower stratosphere, with statistically significant trends being present only in the Southern Hemisphere. Since GHG are well mixed, this asymmetry points to ozone depletion, and hence to ODS emissions, as a key anthropogenic cause of BDC trends in the late twentieth century. More recently, Polvani et al. (2017) have argued that the lack of cooling in the tropical lower stratosphere since the turn of the century (Seidel et al., 2016) contrasted with the substantial cooling in the last two decades of the twentieth century, is a clear indicator that ODS are driving tropical upwelling: recall that both temperature and ozone in the lower stratosphere are closely linked to tropical upwelling through adiabatic cooling and upward advection of low-ozone air, respectively (see, e.g., Abalos et al., 2012).

On the modeling side too, several studies have reported the key role of ODS as drivers of BDC trends. Oman et al. (2009) found ozone depletion to be the major factor causing decreases in age of air (AoA), in their model, in the second half of the twentieth century. Oberländer-Hayn et al. (2015), comparing time-slice model integrations at year 1960 and year 2000 conditions, reported the BDC acceleration caused by ODS over that period to be of equal magnitude to the acceleration caused by GHG. A similar result, but focusing on mean age of stratospheric air, was reported by Li et al. (2018), using time-varying forcings over the period 1960–2010. The importance of ODS emissions for BDC trends in the last few decades was also noted by Garfinkel et al. (2017). And, while seeking to understand the intermodel spread in ozone simulations in the most recent chemistry-Climate Model Intercomparison Project, Morgenstern et al. (2018) found that AoA trends are driven by both GHG and ODS, with increases in the latter driving a decrease in AoA in most models (except over the summer South Pole).

As for the coming decades, Polvani et al. (2018) recently found that AoA trends over the period 2000–2080 will be 4 times smaller than over the period 1960–2000 as a consequence of the Montreal Protocol, adding to earlier work (Lin & Fu, 2013; McLandress et al., 2010; Oberländer et al., 2013). Taken as a whole, these studies offer good evidence that ODS are indeed key forcings of past and future BDC changes. However, these studies comprise a relatively small set of models. Furthermore, since the models were forced in different ways and their output was analyzed over different periods, they cannot be quantitatively compared.

Hence, the goal of this paper is as follows: to quantify the importance of ODS in driving BDC trends, in both past and future decades, using a large number of models with similar forcing scenarios. We also seek to directly contrast the importance of ODS and GHG and to provide an estimate of the uncertainty in the ODS/GHG impact on BDC trends, as we quantify the spread across the models.

Our work builds on the study of Lin and Fu (2013) who analyzed BDC trends in 13 models from the Stratospheric Processes and their Role in Climate/Chemistry-Climate Model Validation project, Phase 2 (hereafter CCMVal-2; Eyring et al., 2008), and discussed the role of ozone depletion/recovery on those trends. We expand on their findings in three ways. First, we here analyze a larger set of models, adding those from the recent Chemistry-Climate Model Initiative, Phase 1 (hereafter CCMI; Eyring et al., 2013; Morgenstern et al., 2017) to the CCMVal-2 models. Second, in addition to the scenarios where *all* forcings vary with time, we examine the sensitivity integrations to identify and contrast the separate impacts of ODS and GHG. And, finally, we here shift the emphasis from ozone to ODS, keeping in mind that ozone is naturally abundant in the atmosphere, and ODS are the anthropogenic emissions that need to be contrasted with GHG.

The paper is laid out as follows. In section 2 we describe the models and the scenario forcings analyzed here. In section 3 we contrast past and future BDC trends: as GHG increase monotonically from the mid-20th century to the end of the 21st century, whereas trends in the concentrations the ODS change sign in the late 1990s as a consequence of the Montreal Protocol, any difference in forced trends before and after the year 2000 can be unambiguously attributed to ODS. In section 4, we exploit the existence of the sensitivity integrations and quantitatively explore the relative importance of ODS and GHG in affecting BDC trends. A summary and discussion close the paper in section 5.

Table 1
The Models Analyzed in This Study and Their Data Availability (Indicated by an X)

	AoA		$\bar{w}^*$	
Model name	All Forcings	Fixed ODS/GHG	All Forcings	Fixed ODS/GHG
		CCMVal-2		
CAM3.5	X		X	
CCSRNIES			X	X
CMAM	X	X	X	X
GEOSCCM	X		X	
LMDZrepro	X		X	X
MPRI	X	X	X	X
NIWA-SOCOL	X		X	
SOCOL	X	X	X	X
UMUKCA-METO	X		X	
UMUKCA-UCAM	X		X	
WACCM	X		X	
		CCMI		
ACCESS CCM			X	
WACCM	X	X	X	X
CMAM	X	X	X	X
CNRM-CM5-3	X			
EMAC L47	X		X	
EMAC L90	X		X	
GEOSCCM	X		X	
HadGEM3-ES	X			
MRI-ESM1r1	X		X	
NIWA-UKCA	X	X	X	X
UMSLIMCAT	X	X		

Note. ODS = ozone-depleting substances; GHG = greenhouse gases; CCMVal-2 = Chemistry-Climate Model Validation project, Phase 2; CCMI = Chemistry-Climate Model Initiative.

2. Methods

We here analyze a total of 20 models for which output was made available, combining both the CCMVal-2 and CCMI projects. These models, listed in Table 1, are extensively documented in Morgenstern et al. (2010) and Morgenstern et al. (2017) for the CCMVal-2 and CCMI projects, respectively. Unless otherwise noted, we consider only one run for each model and scenario, in order to weigh all models equally. In a nutshell, with few exceptions, these are atmospheric general circulation models with a well-resolved stratosphere, that is, with a model top near or above 0.01 hPa. Typical resolutions are 2–3° in latitude/longitude, and 50–90 levels in the vertical direction. It should be noted that all models used here include an interactive chemistry module for stratospheric ozone and, in most CCMI models, comprehensive tropospheric chemistry as well.

Three sets of integrations are considered here, each set corresponding to a different forcing scenario. The first set, which we will refer to as the "All Forcings" integrations, simulate the climate system over the period 1960–2100 with models forced by time-varying concentrations of GHG and ODS. The sea surface temperature and sea ice concentrations (SSTs) are typically prescribed from either observations or model output although, in a few instances, the atmospheric model is fully coupled to interactive ocean and sea ice models. The chemistry-climate modeling projects technically refer to this scenario as the "REF-B2" and "REF-C2," for CCMVal-2 and CCMI, respectively (Eyring et al., 2008, 2013).

The anthropogenic forcings used for these All Forcings scenarios are quite similar between CCMVal-2 and CCMI, but not exactly identical. For ODS, both REF-B2 and REF-C2 prescribe them following the same A1 scenario (World Meteorological Organization, 2011), but for GHG the specifications are a little different. The newer REF-C2 models follow the RCP6.0 scenario (Meinshausen et al., 2011) for GHG, whereas the

older REF-B2 models follow the SRES A1B scenario (Nakicenovic et al., 2000). Fortunately, this is not too problematic, as RCP6.0 and SRES A1B forcings from CO_2 and N_2O are very similar between 1960 and 2100. As noted in Morgenstern et al. (2017), the main discrepancy is found in CH_4 forcing, whose volume mixing ratio peaks at about 2.4 ppmv in the late 21st century for REF-B2, but only at 1.95 ppmv for the REF-C2 forcings. To the degree that CO_2 constitutes the bulk of GHG forcing, this 20% discrepancy in methane is a minor issue, as it results in a total radiative difference in GHG forcing of a few percent between CCMVal-2 and CCMI.

The other two sets of model integrations analyzed here are used to *quantitatively* establish the respective contributions of ODS and GHG. These sets follow scenarios in which either ODS or GHG are kept fixed at year 1960 levels, all else being identical (except for the SSTs which, for consistency, are also kept at ~1960 levels when GHG are fixed, in models with prescribed SSTs). In these paper we refer to these sets of integrations as the *single-fixed-forcing* runs, because that expression immediately conveys the idea that only one forcing is being altered; a more precise expression would be *all-but-one-forcing*, but that is unnecessarily cumbersome. For maximum clarity these two sets are here referred to as the "Fixed ODS" and "Fixed GHG" integrations. And, for the sake of full reproducibility, we note that these integrations correspond to the SCN-B2b and SCN-B2c scenario runs of the CCMVal-2 project (Eyring et al., 2008), and the SEN-C2-fODS and SEN-C2-fGHG scenario runs of the CCMI project (Eyring et al., 2013), respectively.

The effects of ODS (or GHG) on the BDC are here quantified by computing differences between the All Forcings runs and Fixed ODS (or GHG) runs. Note that in the Fixed ODS runs both the effect of ODS on the ozone layer and the radiative effect of ODS remain constant with time. We are here unable to separately quantify the importance of these two mechanisms for BDC trends, as ozone is not prescribed independently of ODS in these models (it is computed interactively). However, as originally noted in Polvani et al. (2018), and as we will show below for the CCMI models, the effects of ODS on BDC trends exhibit clear seasonal and hemispheric asymmetries that are aligned with ozone changes, indicating that the direct radiative forcing of ODS is relatively unimportant for BDC trends. We have recently confirmed this fact using the Whole Atmosphere Community Climate Model (WACCM), as detailed in Abalos et al. (2019).

Unfortunately, the majority of models participating in the CCMVal-2 and CCMI projects did not contribute model output for the single-fixed-forcing scenario integrations. In fact, as shown in Table 1, only a handful of models for each project contributed data for the two variables of interest here: the mean AoA and the residual vertical velocity ($\bar{w}^*$). To obtain the strongest possible results, therefore, we decided to combine model output from the two projects. The models themselves are quite similar, basically one generation apart at most, and so are the forcings, as explained above.

Finally, unlike CO_2 concentrations, ODS concentrations are *not* monotonically increasing from 1960 to 2100. Hence, it is crucial to consider *separately* the pre- and post-Montreal Protocol periods, as it makes little sense to compute a single linear trend in model responses over periods during which the forcing trends change sign. Since the ozone-depleting power of ODS—as quantified by equivalent effective stratospheric chlorine (see, e.g., Newman et al., 2007)—peaked around 1998, we follow Polvani et al. (2018) and simply choose the year 2000 as the break point. Unlike that study, however, we are here forced to select the shorter 1980–2000 period for the pre-Montreal trends, since the AoA tracer needs at least a decade or two to come into equilibrium, and the model integrations were started around 1960. For the post-Montreal period we follow Polvani et al. (2018) and use 2000–2080, to avoid the reversal of CH_4 trends in the forcing scenarios in the final decades of the 21st century. For simplicity we will refer to 1980-2000 and 2000-2080 as "the past" and "the future," respectively, in the remainder of the paper.

3. Past and Future Impact of ODS on BDC Trends

The main goal of our paper is to bring out the effect of ODS on the BDC and for this the single-fixed-forcing runs are crucial. However, we postpone analyzing those to the next section, as it is instructive to start by looking at the All Forcings runs. We do this for two reasons. First, we have many more models available for the All Forcings runs than for the single-fixed-forcing runs (see Table 1). Second, the All Forcings runs are the most realistic simulations available and thus represent the closest model approximation to the actual atmospheric evolution.

As it happens, it is relatively easy to bring out the role of ODS in the All Forcings runs, since only ODS trends change dramatically around the year 2000, whereas GHG trends do not change sign at that time (and,

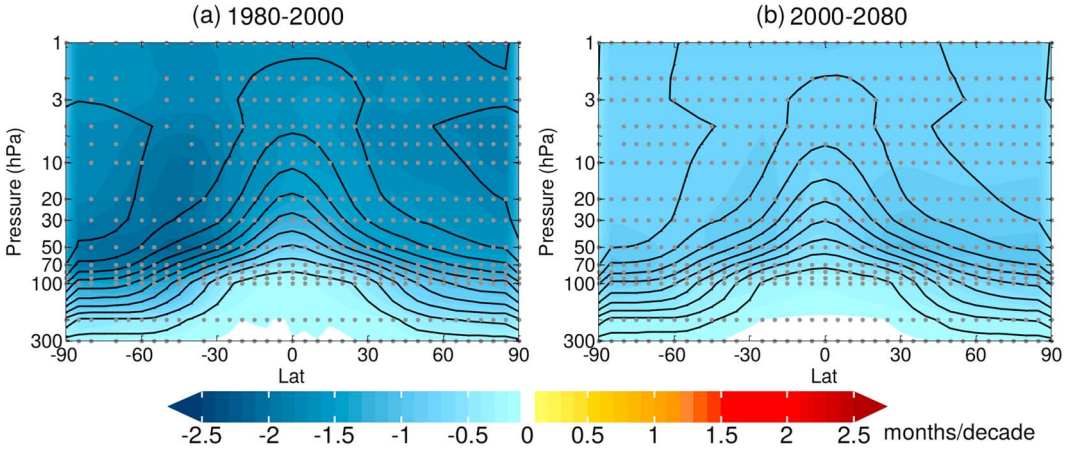

Figure 1. Multimodel mean, annual mean trends (shading), and climatology (contours) of age of air for the All Forcings runs (combined Chemistry-Climate Model Validation project, Phase 2, REF-B2 and Chemistry-Climate Model Initiative REF-C2) for (a) 1980–2000 and (b) 2000–2080. The stippling represents the trends significant at the 95% interval by a two-tailed *t* test. For the climatology, the contour interval is 6 months; the zero contour is not shown.

in fact, at no other time over the period of interest). Assuming internal decadal variability to be relatively small in the stratosphere (we will illustrate this later in the paper), any changes in BDC trends before/after the year 2000 can therefore be immediately attributed to changes in ODS concentrations, and thus to the Montreal Protocol. A similar approach was used in Barnes et al. (2014) to bring out the ODS impacts on the tropospheric circulation and surface climate in the All Forcings simulations of the models that participated in the Climate Model Intercomparison Project, Phase 5 (Taylor et al., 2012).

We start, therefore, by simply contrasting the past and future AoA trends, computed using simple linear regression, for the All Forcings integrations of 20 models in Table 1: the multimodel mean values are shown in the left and right panels of Figure 1, for the past and future periods, respectively. It is immediately clear from the color difference that future AoA trends are substantially smaller than past trends, and this can be directly attributed to the phaseout of ODS emissions by the Montreal Protocol. Quantitatively speaking, as reported in the top row of Table 2, we find that future AoA trends will be less than half the values of past trends.

To give a sense of the spread across models, we plot in Figure 2 the past and future AoA trends for each of the 20 models analyzed. We show the annual mean, global mean AoA trends, averaged over the 100–1 hPa layer, on the left panel: the solid bars show the past trends, the empty bars the future trends. For clarity, the ratio of past to future trends is shown by the black bars in the right panel. With a few exceptions, the vast majority of the models show a clear reduction in AoA trends, confirming the original finding of Polvani et al. (2018), who used the CCMI-WACCM model. That model appears to show the strongest reduction. It is important, however, to keep in mind that only one run for each model was used in Figure 2 (in order to

Table 2
Past and Future, Multimodel (With the Number of Models in Parenthesis) Average of Annual and Global Mean AoA Trends, Vertically Averaged Between 1 and 100 hPa, in Units of Years per Decade

AoA trends (years per decade)	Past (1980–2000)	Future (200–2080)
All Forcings (20)	−0.118 ± 0.033	−0.052 ± 0.006
All Forcings (7)	−0.117 ± 0.035	−0.041 ± 0.005
Fixed ODS (7)	−0.053 ± 0.037	−0.055 ± 0.006
Fixed GHG (7)	−0.071 ± 0.037	0.009 ± 0.005

Note. All values are statistically significant at the 95% confidence interval by a two-tailed *t* test (with bounds indicated after the ± symbols). The seven models in the last three rows are those for which the single-fixed-forcing integrations are also available (see Table 1). AoA = age of air; ODS = ozone-depleting substances; GHG = greenhouse gases.

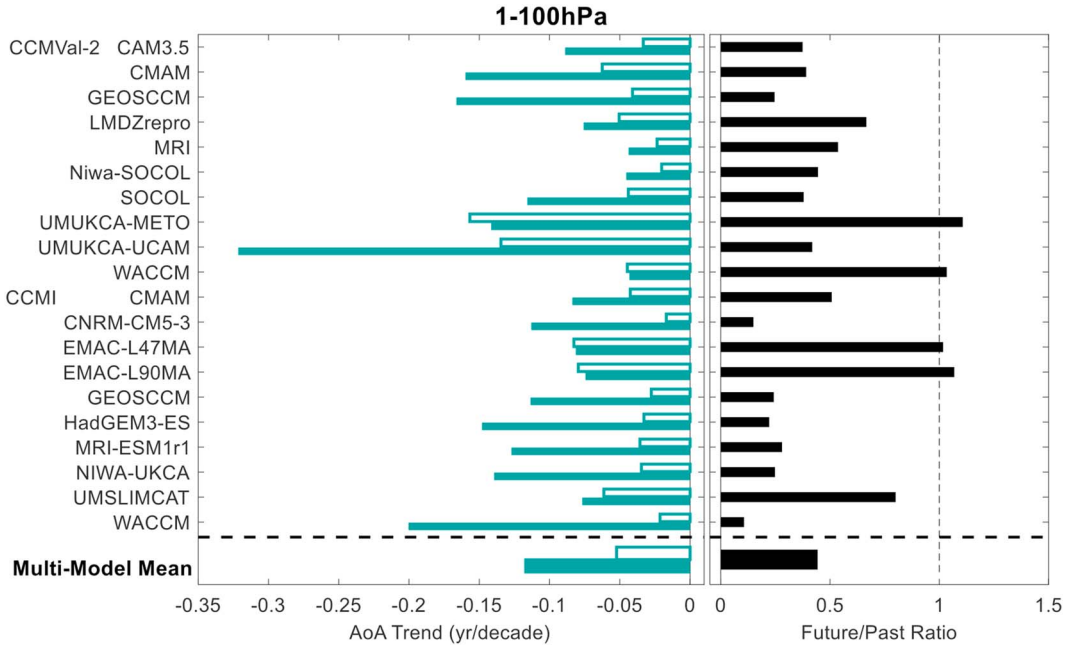

Figure 2. Past (1980–2000; filled green bars) and future (2000–2080; empty green bars) global-mean and annual-mean AoA trends (left) and their ratio (right), vertically averaged between 100 and 1 hPa for CCMVal-2 REF-B2 and CCMI REF-C2 (All Forcings) simulations. CCMVal-2 = Chemistry-Climate Model Validation project, Phase 2; CCMI = Chemistry-Climate Model Initiative; AoA = age of air.

weigh all the models equally). Hence, one cannot determine the relative amplitude of the forced response in the models from this figure, as internal variability may be large, and needs to be removed by averaging several runs. The role of internal variability will be discussed in section 4 below.

In addition to the past/future differences, one can exploit the strong seasonal cycle and hemispheric asymmetry of ozone depletion to bring out the key role of ODS on past and future BDC trends. As noted by Polvani et al. (2018), the impact of ODS is primarily (but not uniquely) mediated by the formation of the ozone hole. Although such ODS impact is sufficiently large to survive averaging over all months of the year, as we have just shown, it can be greatly amplified by considering the hemispheric and seasonal asymmetries. We illustrate these in Figure 3, where the multimodel mean, zonal mean trends for the residual vertical velocity w^* are shown (the gray stippling is used to mark regions where trends are statistically significant). The climatology is shown by the black contours, solid indicating upwelling (in the tropics) and dashed downwelling (at high latitudes), separated by the dash-dotted zero contour.

Let us start by considering the top left panel, which shows the *annual* mean $\bar{w}^*$ trends for the past period: recall that these trends are computed from the realistic All Forcings simulations. For that period, only the Southern Hemisphere shows large statistically significant trends at high latitudes. This hemispheric asymmetry points to ODS, not GHG, since the latter are well mixed. This is confirmed by the middle and bottom left panels, which show the *seasonal* December–February (DJF) and June–August (JJA) trends over the same period. It is clear that the large BDC trends—the increased downwelling at high southern latitudes—come from austral summer, the season where ozone depletion is known to mostly affect the atmospheric circulation, as widely documented in the literature (see, e.g., Figure 4 of Polvani et al., 2018).

The large role of ODS on the BDC is further confirmed by contrasting past and future $\bar{w}^*$ trends. Starting from the annual mean in the top row, one can see a very large hemispheric asymmetry in future trends (right panel): whereas the tropics show increased upwelling and the northern high latitudes increased downwelling, as one expects from increases in GHG, the southern high latitudes show *reduced downwelling*. This deceleration of the BDC over the South Pole in the 21st century comes mostly from DJF, as seen the middle right panel. We can easily attribute it, therefore, to the closing of the ozone hole, and thus to reduced ODS concentrations. The future DJF trends are very different from the JJA ones, shown in the bottom right panel:

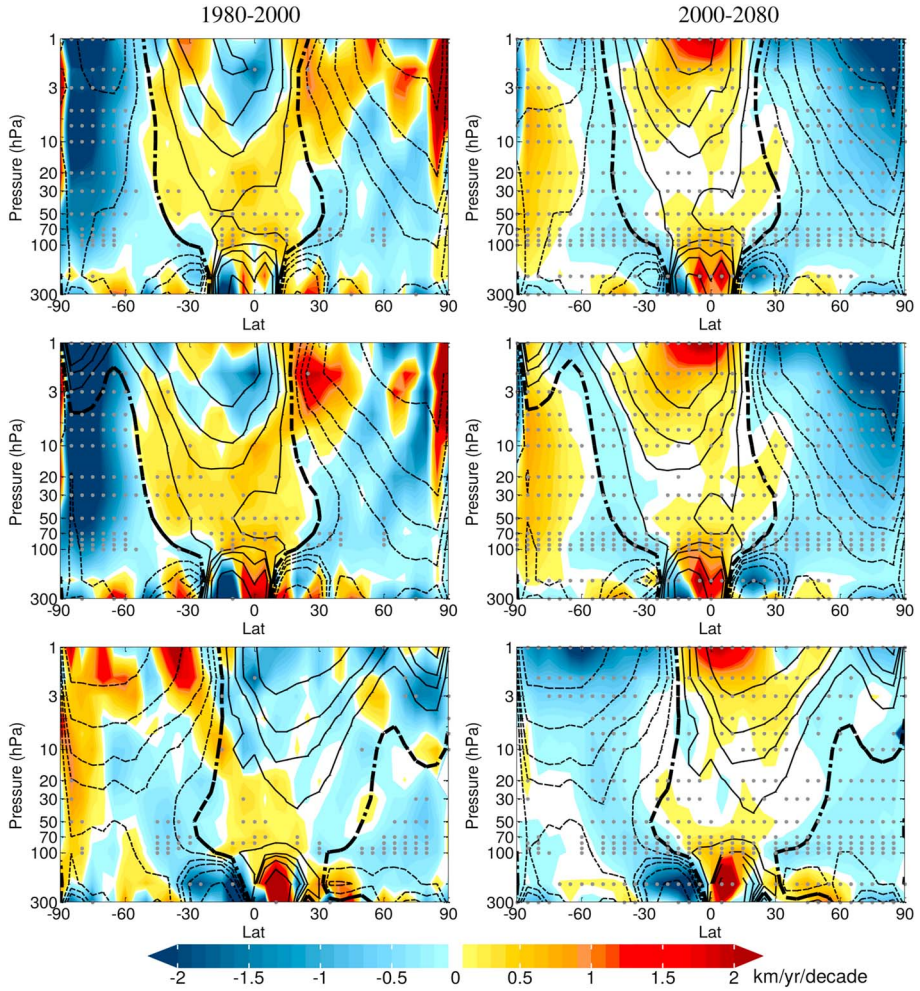

Figure 3. Past (left) and future (right) multimodel mean, zonal mean $\bar{w}^*$ trends (shading) in the annual (top row), December–February (middle row), and June–August (bottom row) means. The black contours show the corresponding climatology, with contour lines at −100, −50, −30, −20, −10, 0, 10, 20, 30, 50, and 100 km/year, positive in solid, zero in dash dotted, and negative in dashed. The gray stippling shows where trends are significant at the 95% interval, using a two-tailed *t* test.

in austral winter, when GHG are the key forcing, we see a BDC acceleration at the southern high latitudes as well as in the tropics, as expected.

4. The Relative Importance of ODS and GHG for BDC Trends

As we have shown, the large impact of ODS on BDC trends in the All Forcings runs, both for the past and for the future, is readily apparent from the seasonal and hemispheric asymmetries associated with the opening/closing of the ozone hole, which is the primary pathway through which ODS affect the BDC. In those runs, however, it is not possible to quantify the relative importance of the ODS and GHG forcings. To do that, we need to analyze the single-fixed-forcing runs, which we explore in this section. Unfortunately, even after combining the CCMVal-2 and CCMI project, AoA output is available for only seven models (and eight models for $\bar{w}^*$; see Table 1). While not a huge set, this is sufficient to gain a first impression of the relative importance of ODS and GHG forcings from a multimodel perspective.

We start by discussing the AoA trends, past and future, shown for the single-fixed-forcing and the All Forcings runs in Figure 4. Let us first consider the past trends (1980–2000), which are illustrated by the solid bars. One can see that, in most models, the AoA trends in the Fixed GHG runs (orange solid bars) are comparable to the trends in the Fixed ODS runs (magenta bars). In the multimodel mean, the past impact of ODS appears to be somewhat larger than the impact of GHG (by about 30%; see Table 2), but that difference

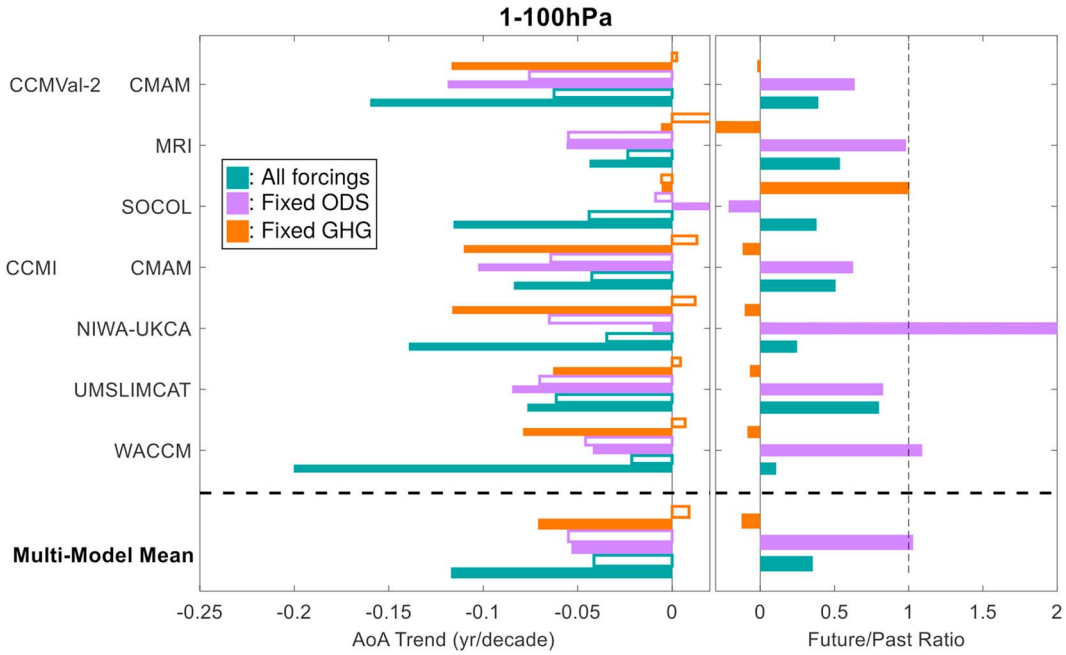

Figure 4. (left) Past (1980–2000; filled bars) and future (2000–2080; empty bars) global-mean, zonal-mean, and annual-mean AoA trends, vertically averaged between 100 and 1 hPa for CCMVal-2 and CCMI simulations for All Forcings (green), Fixed ODS (magenta), and Fixed GHG (orange) scenarios. (right) Future/past trend ratio for each scenario, color coded as in the left panel. ODS = ozone-depleting substances; GHG = greenhouse gases; CCMVal-2 = Chemistry-Climate Model Validation project, Phase 2; CCMI = Chemistry-Climate Model Initiative; AoA = age of air.

is not statistically significant, due to the spread across models. We conclude that ODS and GHG have contributed *in roughly equal parts* to the past AoA trends: this confirms the recent studies of Oberländer-Hayn et al. (2015) and Li et al. (2018), who used different models and different periods.

Next, we contrast future and past trends, in the single forcing runs. Consider the empty orange bars in the left panel, and note that they are *negative* for six of the seven models analyzed here. As GHG concentrations are fixed for those runs, it is the ODS reversal as a consequence of the Montreal Protocol that causes AoA to increase over the period 2000–2080 in those runs. This ODS forcing, then, opposes the continuous AoA decrease caused by increasing GHG amounts (empty purple bars). This results in future trends that are considerably smaller than in the past, as one can see by contrasting the empty and solid green bars. This multimodel analysis, therefore, confirms the findings reported by Polvani et al. (2018).

Finally, the right panel of Figure 4 shows the future/past trend ratio. For the All Forcings runs, the multimodel mean ratio is 0.35 (see Table 2), a reduction of trends by nearly two thirds (for this smaller subset of seven models), as the reversed ODS trends cancel the effect of increasing GHG. Finally, as a sanity check, note from the purple bar that the future/past ratio for the Fixed ODS runs is very close to one in the multimodel mean, as one might expect when GHG are the sole forcing acting on the stratospheric circulation, since GHG concentrations increase almost linearly in the scenarios used to force these model runs.

To appreciate that the results presented here are not fundamentally dependent on our choice of past/future periods, we show the entire time series of AoA for two of the models in Table 1: the Canadian Middle Atmosphere Model (CMAM, Grandpré et al., 2000; McLandress et al., 2010; Scinocca et al., 2008) and the WACCM (Garcia et al., 2017; Marsh et al., 2013; Solomon et al., 2015). For these two models, runs are available for all the scenario forcings and, more importantly, a *small ensemble* of three runs is available for each scenario. To be clear, each member of these small ensembles is identically forced (according to the appropriate scenario), and the only difference between the three members resides in a very small perturbation in the model's initial condition, in the spirit of Deser et al. (2012). This allows us to quantify the importance of internal variability and determine to what degree it is able to alter the forced response of the BDC to the various forcings.

The complete 1960–2100 time series of AoA are shown in Figure 5, for CMAM and WACCM, on the left and right panels, respectively. The colors indicate the different scenarios, as shown in the legend. First, in the

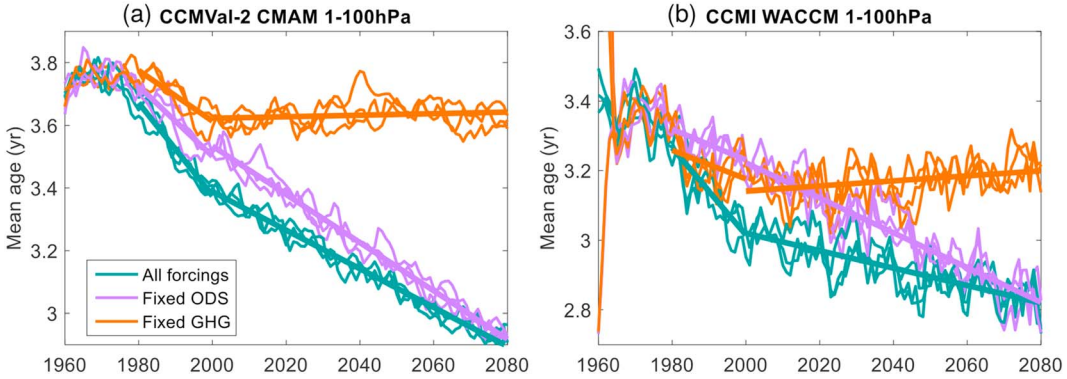

Figure 5. Annual and global mean AoA time series averaged over 100–1 hPa for (a) CCMVal-2 CMAM and (b) CCMI WACCM. Three ensemble members are show in thin curves for each scenario, while the 1980–2000 and 2000–2080 linear trends of the ensemble mean are plotted in thick lines. Color coding as per the caption, consistent with Figure 4. CCMVal-2 = Chemistry-Climate Model Validation project, Phase 2; CCMI = Chemistry-Climate Model Initiative; WACCM = Whole Atmosphere Community Climate Model; CMAM = Canadian Middle Atmosphere Model; ODS = ozone-depleting substances; GHG = greenhouse gases.

All Forcings runs (green curves) one can see a clear kink around the year 2000: this abrupt change in slope, of course, is due to ODS emission and is readily apparent in the orange curves showing the runs with GHG fixed at 1960 levels and only ODS concentrations varying in time. Second, in the absence of ODS forcing (red curves) one can see that AoA increases almost linearly from 1960 all the way to 2100, as GHG concentrations increase monotonically over the entire 140-year period. Third, the area between the green and purple lines quantifies the impact of ODS on AoA trends: it is clear that the quantitative impact is model dependent (larger in WACCM than in CMAM), and this very fact motivates the present study. In both cases, however, we see that the green curves are steeper than the purple curves before 2000, and less steep after 2000. This is the effect of ODS on the BDC, which is robust across models. Finally, a technical note: Figure 5 shows that AoA does not vary linearly prior to 1980. This is because it takes time for tracer to become equilibrated throughout the entire stratosphere and for the forced response to emerge from internal variability, hence our choice to evaluate the past trends starting at 1980 in these runs.

A second important result can be gathered from in Figure 5. Notice that for both models, and for each forcing scenario, the three members of each ensemble track each other quite closely. From this we conclude that for multidecadal BDC trends the role of internal variability appears to be relatively small in these models. For short periods, needless to say, the actual numerical value of trends can vary considerably across different ensemble members of the same model: for instance, for the 1980–2000 period, the AoA trends for the three WACCM members in Figure 5 are −0.200, −0.096, and −0.079 years per decade, showing a considerable spread. This suggests that a substantial fraction of the intermodel spread seen in Figure 2 might arise from internal variability, rather than from intrinsic model differences. Nevertheless, Figure 5 clearly suggests that large ensembles may not be needed to robustly quantify AoA trends, as is the case, for instance, for the global mean surface temperature (Deser et al., 2012).

We conclude by illustrating the entire vertical structure $\bar{w}^*$ trends in the tropics, to highlight the key role of ODS on tropical upwelling, as suggested by Polvani et al. (2017) on the basis of satellite temperature observations. Trends in $\bar{w}^*$ from 100 to 5 hPa, averaged between the turnaround latitudes (i.e., over the region of tropical upwelling), are plotted in Figure 6, for each of the forcing scenarios, and averaged across the eight models for which output is available for all scenarios (see Table 1). In each panel we plot one curve for the past trends (solid) and one for the future trends (dashed), with the shaded envelope indicating the 95% confidence interval from a two-tailed t test.

Let us start with the top row, where the DJF trends are shown. In the All Forcings simulations (left panel) one can see that tropical upwelling in the future is considerably smaller than in the past, over most of the stratospheric column. The large values of past trends are due, to a considerable extent, to ODS: this is seen by the fact that when the ODS forcing is absent (middle top panel), GHG alone are not sufficient to yield a statistically significant trends (Lamarque & Solomon, 2010). Furthermore, the top left panel shows that DJF upwelling trends caused by ODS reverse sign after the year 2000, again over the entire stratospheric

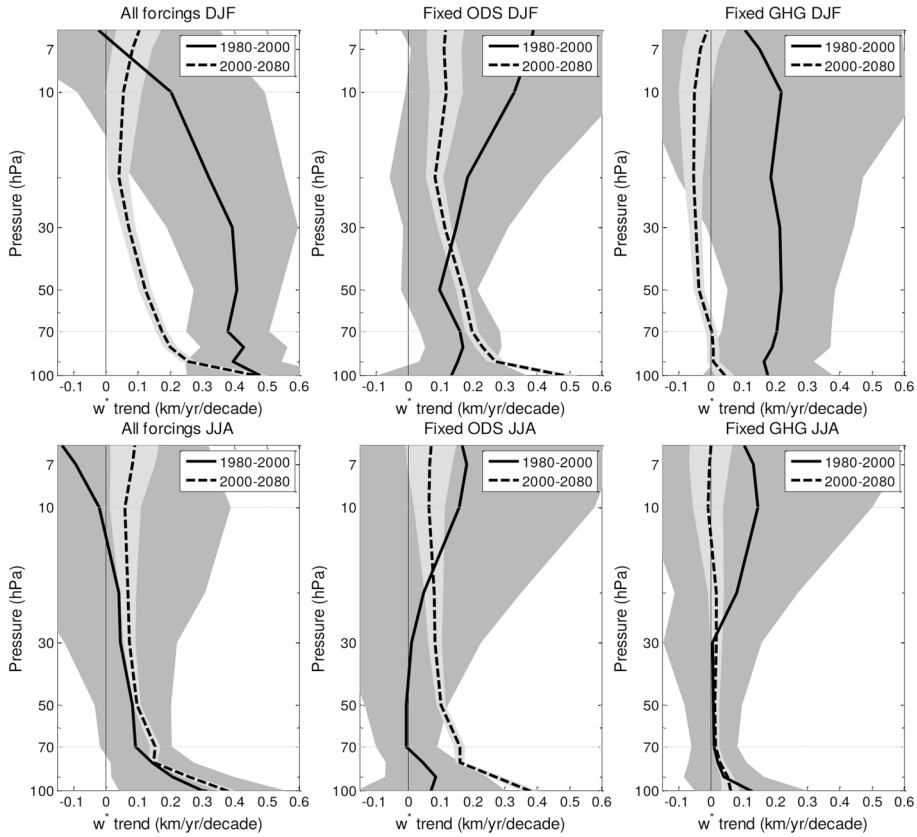

Figure 6. Vertical profile of multimodel (CCMVal-2 + CCMI: eight models) mean seasonal trends of $\bar{w}^*$ in DJF (top row) and JJA (bottom row) for the periods of 1980–2000 (solid) and 2000–2080 (dashed) for three scenarios: All Forcings (left column), Fixed ODS (middle column), and Fixed GHG (right column). Here $\bar{w}^*$ is computed by averaging over the tropical upwelling zone, that is, between the turning points, of the corresponding season. ODS = ozone-depleting substances; GHG = greenhouse gases; CCMVal-2 = Chemistry-Climate Model Validation project, Phase 2; CCMI = Chemistry-Climate Model Initiative; JJA = June–August; DJF = December–February.

column: as a consequence the overall future DJF trends are severely reduced. Finally, the corresponding JJA trends are shown in the bottom row: for the future, statistically significant trends are seen in the All Forcings simulations, and these come almost entirely from GHG (contrast the lower middle and left panels). Interestingly enough, past trends are not statistically significant in that season: the GHG forcing alone, over the relatively short 1980–2000 period (only two decades) is not sufficient to produce a significant response. It is only in DJF, when the ODS contribute a substantial forcing, that a statistically significant trend is seen in these models.

5. Summary and Discussion

Using a large set of chemistry-climate models, forced in a consistent manner and analyzed over identical time periods (for the past and for the future, separately), we have shown that ODS are important drivers of trends in the stratospheric circulation. We have found that ODS have contributed at least 50% of the forced response in the late twentieth century, confirming the results of several earlier single-model studies (Li et al., 2018; Oberländer-Hayn et al., 2015; Oman et al., 2009; Polvani et al., 2018). Furthermore, in the coming decades, the banning of ODS by the Montreal Protocol will result in much reduced BDC trends, roughly half of the value up to the year 2000 when chlorine levels peaked in the stratosphere.

While the attribution of modeled trends to ODS concentrations in our study is completely unequivocal since we have made use of single-fixed-forcing runs, the precise mechanism via which ODS impact the BDC will need further study. To a large degree, ODS act via the formation of the ozone hole: the resulting large perturbations to the temperature affects atmospheric waves which, upon breaking, drive the BDC. This is why the largest ODS signals are found in DJF and in the Southern Hemisphere. However, it is not immediately

obvious how to convert a perturbation in the lower stratospheric temperature gradient (resulting from the formation of the ozone hole) into a change in the wave flux divergence; that is, we have no theory for computing one from the other a priori: all we can do is to diagnose model output. In the case of increasing GHG, Eichelberger and Hartmann (2005) have argued, from numerical experiments with a simple dynamical-core model, that tropical tropospheric warming caused by higher concentrations of GHG results in a larger meridional temperature gradient at midlatitudes, which increases baroclinicity, which increases wave activity at synoptic and planetary scales, and eventually yields a stronger BDC. More recently, Shepherd and McLandress (2011) have argued that increasing GHG alter the location of critical layers on the tropical lower stratosphere resulting in more upward wave propagation and thus a stronger BDC. Whether similar mechanisms are at work in the case of ODS forcings remains to be determined. The key difference with GHG is that the temperature gradients caused by ODS are mostly in the lower stratosphere, and not in the troposphere. In addition, it is well known that ODS act as GHG (see, e.g., Velders et al., 2007), and their impact on the stratospheric circulation might partly be mediated by SST changes.

Another important question should also be explored in future studies. In the coming decades, the degree of trend cancelation between the decreasing ODS and increasing GHG will very likely depend on the scenario used. For example, regarding the poleward shift of the tropospheric eddy-driven jet in the Southern Hemisphere, Barnes et al. (2014) showed that the levels of CO_2 will be crucial in determining the extent of the shift in austral summer: in the RCP2.6 scenario recovery of stratospheric ozone will result in a net *equatorward* shift of the eddy-driven jet, whereas the jet will shift *poleward* in the RCP8.5 scenario. Without running a model with different forcing scenarios, it is impossible to determine the sign of future BDC trends. However, it is not inconceivable that in a weak forcing scenario, such as RCP2.6, the recovery of stratospheric ozone might actually overwhelm the increasing CO_2 forcing and result in a net deceleration of the BDC into the late 21st century. We hope future model intercomparison projects with chemistry-climate models will address this issue by exploring different scenarios.

Acknowledgments

L. M. P. is most grateful for the hospitality of the Wartner family and the entire staff of the Eurotel Victoria in Les Diablerets, Switzerland, where the bulk of this manuscript was penned. He also acknowledges the continued support by the U.S. National Science Foundation (NSF). L. W. is supported by Grant JIH2308109 from Fudan University and Grant 41875047 from National Natural Science Foundation of China (NSFC). M. A. acknowledges funding from the Program Atraccion de Talento de la Comunidad de Madrid (2016-T2/AMB-1405) and the Spanish National Project STEADY (CGL2017-83198-R). N. B. was supported by the Met Office Hadley Centre Programme funded by BEIS and Defra and by the European Commission's Seventh Framework Programme StratoClim Project 226520. This research was also supported by the NZ Governments Strategic Science Investment Fund (SSIF) through the NIWA program CACV, and O. M. acknowledges funding by the New Zealand Royal Society Marsden Fund (Grant 12-NIW-006). Furthermore, Gang Zeng (from NIWA) performed the NIWA-UKCA simulations used in this study. All the data used here are publicly available via the CCMVal-2 and CCMI projects, as detailed in Morgenstern et al. (2010) and Morgenstern et al. (2017).

References

Abalos, M., Polvani, L. M., Calvo, N., Kinnison, D., Ploeger, F., Randel, W. J., & Solomon, S. (2019). New insights on the impact of ozone depleting substances on the Brewer-Dobson circulation. *Journal of Geophysical Research: Atmospheres*, *124*, 2435–2451. https://doi.org/10.1029/2018JD029301

Abalos, M., Randel, W., & Serrano, E. (2012). Variability in upwelling across the tropical tropopause and correlations with tracers in the lower stratosphere. *Atmospheric Chemistry and Physics*, *12*(23), 11,505–11,517.

Barnes, E. A., Barnes, N. W., & Polvani, L. M. (2014). Delayed southern hemisphere climate change induced by stratospheric ozone recovery, as projected by the CMIP5 models. *Journal of Climate*, *27*(1), 853–867.

Brewer, A. W. (1949). Evidence for a world circulation provided by the measurements of helium and water vapour distribution in the stratosphere. *Quarterly Journal of the Royal Meteorological Society*, *75*(326), 351–363.

Butchart, N., Cionni, I., Eyring, V., Shepherd, T., Waugh, D., Akiyoshi, H., et al. (2010). Chemistry–climate model simulations of twenty-first century stratospheric climate and circulation changes. *Journal of Climate*, *23*(20), 5349–5374.

Butchart, N., & Scaife, A. A. (2001). Removal of chlorofluorocarbons by increased mass exchange between the stratosphere and troposphere in a changing climate. *Nature*, *410*(6830), 799–802.

Butchart, N., Scaife, A., Bourqui, M., De Grandpré, J., Hare, S., Kettleborough, J., et al. (2006). Simulations of anthropogenic change in the strength of the Brewer-Dobson circulation. *Climate Dynamics*, *27*(7-8), 727–741.

Deser, C., Phillips, A., Bourdette, V., & Teng, H. (2012). Uncertainty in climate change projections: The role of internal variability. *Climate Dynamics*, *38*(3), 527–546.

Dobson, G. M., Harrison, D., & Lawrence, J. (1929). Measurements of the amount of ozone in the Earth's atmosphere and its relation to other geophysical conditions. Part III. *Proceedings of the Royal Society of London. Series A, Containing Papers of a Mathematical and Physical Character*, *122*(790), 456–486.

Eichelberger, S. J., & Hartmann, D. L. (2005). Changes in the strength of the Brewer-Dobson circulation in a simple AGCM. *Geophysical research letters*, *32*, L15807. https://doi.org/10.1029/2005GL022924

Eyring, V., Chipperfield, M. P., Giorgetta, M. A., Kinnison, D. E., Matthes, K., Newman, P. A., et al. (2008). Overview of the new CCMval reference and sensitivity simulations in support of upcoming ozone and climate assessments and the planned SPARC CCMVal report. *SPARC Newsletter*, *30*, 20–26.

Eyring, V., Lamarque, J.-F., Hess, P., Arfeuille, F., Bowman, M. P., Chipperfield, K., et al. (2013). Overview of IGAC/SPARC Chemistry-Climate Model Initiative (CCMI) community simulations in support of upcoming ozone and climate assessments. *SPARC Newsletter*, *40*, 48–66.

Fu, Q., Lin, P., Solomon, S., & Hartmann, D. L. (2015). Observational evidence of strengthening of the Brewer-Dobson circulation since 1980. *Journal of Geophysical Research: Atmospheres*, *120*, 10,214–10,228. https://doi.org/10.1002/2015JD023657

Garcia, R. R., & Randel, W. J. (2008). Acceleration of the Brewer-Dobson circulation due to increases in greenhouse gases. *Journal of the Atmospheric Sciences*, *65*(8), 2731–2739.

Garcia, R. R., Smith, A. K., Kinnison, D. E., Cámara, Á. D. L., & Murphy, D. J. (2017). Modification of the gravity wave parameterization in the Whole Atmosphere Community Climate Model: Motivation and results. *Journal of the Atmospheric Sciences*, *74*(1), 275–291.

Garfinkel, C. I., Aquila, V., Waugh, D. W., & Oman, L. D. (2017). Time-varying changes in the simulated structure of the Brewer–Dobson circulation. *Atmospheric Chemistry and Physics*, *17*(2), 1313–1327.

Grandpré, J. D., Beagley, S., Fomichev, V., Griffioen, E., McConnell, J., Medvedev, A., & Shepherd, T. (2000). Ozone climatology using interactive chemistry: Results from the Canadian Middle Atmosphere Model. *Journal of Geophysical Research*, *105*(D21), 26,475–26,491.

Hardiman, S. C., Butchart, N., & Calvo, N. (2014). The morphology of the Brewer-Dobson circulation and its response to climate change in CMIP5 simulations. *Quarterly Journal of the Royal Meteorological Society*, *140*(683), 1958–1965.

Lamarque, J.-F., & Solomon, S. (2010). Impact of changes in climate and halocarbons on recent lower stratosphereozone and temperature trends. *Journal of Climate*, *23*, 2599–2611.

Li, F., Newman, P., Pawson, S., & Perlwitz, J. (2018). Effects of greenhouse gas increase and stratospheric ozone depletion on stratospheric mean age of air in 1960–2010. *Journal of Geophysical Research: Atmospheres*, *123*, 2098–2110. https://doi.org/10.1002/2017JD027562

Lin, P., & Fu, Q. (2013). Changes in various branches of the Brewer–Dobson circulation from an ensemble of chemistry climate models. *Journal of Geophysical Research: Atmospheres*, *118*, 73–84. https://doi.org/10.1029/2012JD018813

Marsh, D. R., Mills, M. J., Kinnison, D. E., Lamarque, J.-F., Calvo, N., & Polvani, L. M. (2013). Climate change from 1850 to 2005 simulated in CESM1 (WACCM). *Journal of Climate*, *26*(19), 7372–7391.

McLandress, C., Jonsson, A. I., Plummer, D. A., Reader, M. C., Scinocca, J. F., & Shepherd, T. G. (2010). Separating the dynamical effects of climate change and ozone depletion. Part I: Southern Hemisphere stratosphere. *Journal of Climate*, *23*(18), 5002–5020.

Meinshausen, M., Smith, S. J., Calvin, K., Daniel, J. S., Kainuma, M., Lamarque, J., et al. (2011). The RCP greenhouse gas concentrations and their extensions from 1765 to 2300. *Climatic Change*, *109*(1-2), 213–241.

Morgenstern, O., Giorgetta, M., Shibata, K., Eyring, V., Waugh, D., Shepherd, T., et al. (2010). Review of the formulation of present-generation stratospheric chemistry-climate models and associated external forcings. *Journal of Geophysical Research*, *115*, D00M02. https://doi.org/10.1029/2009JD013728

Morgenstern, O., Hegglin, M. I., Rozanov, E., O'Connor, F. M., Abraham, N. L., Akiyoshi, H., et al. (2017). Review of the global models used within Phase 1 of the Chemistry-Climate Model Initiative (CCMI). *Geoscientific Model Development*, *10*(2), 639–671.

Morgenstern, O., Stone, K. A., Schofield, R., Akiyoshi, H., Yamashita, Y., Kinnison, D. E., et al. (2018). Ozone sensitivity to varying greenhouse gases and ozone-depleting substances in CCMI-1 simulations. *Atmospheric Chemistry and Physics*, *18*(2), 1091–1114.

Nakicenovic, N., Alcamo, J., Grubler, A., Riahi, K., Roehrl, R., Rogner, H.-H., & Victor, N. (2000). *Special Report on Emissions Scenarios (SRES): A special report of Working Group III of the Intergovernmental Panel on Climate Change*. Cambridge: Cambridge University Press.

Newman, P. A., Daniel, J. S., Waugh, D. W., & Nash (2007). A new formulation of equivalent effective stratospheric chlorine (EESC). *Atmospheric Chemistry and Physics*, *7*, 4537–4552.

Oberländer, S., Langematz, U., & Meul, S. (2013). Unraveling impact factors for future changes in the Brewer-Dobson circulation. *Journal of Geophysical Research: Atmospheres*, *118*, 10,296–10,312. https://doi.org/10.1002/jgrd.50775

Oberländer-Hayn, S., Meul, S., Langematz, U., Abalichin, J., & Haenel, F. (2015). A chemistry-climate model study of past changes in the Brewer-Dobson circulation. *Journal of Geophysical Research: Atmospheres*, *120*, 6742–6757. https://doi.org/10.1002/2014JD022843

Oman, L., Waugh, D. W., Pawson, S., Stolarski, R. S., & Newman, P. A. (2009). On the influence of anthropogenic forcings on changes in the stratospheric mean age. *Journal of Geophysical Research*, *114*, D03105. https://doi.org/10.1029/2008JD010378

Polvani, L. M., Abalos, M., Garcia, R., Kinnison, D., & Randel, W. J. (2018). Significant weakening of Brewer-Dobson circulation trends over the 21st century as a consequence of the Montreal Protocol. *Geophysical Research Letters*, *45*, 401–409. https://doi.org/10.1002/2017GL075345

Polvani, L. M., Wang, L., Aquila, V., & Waugh, D. W. (2017). The impact of ozone-depleting substances on tropical upwelling, as revealed by the absence of lower-stratospheric cooling since the late 1990s. *Journal of Climate*, *30*(7), 2523–2534.

Rind, D., Suozzo, R., Balachandran, N., & Prather, M. (1990). Climate change and the middle atmosphere. Part I: The doubled CO_2 climate. *Journal of the Atmospheric Sciences*, *47*(4), 475–494.

Scinocca, J., McFarlane, N., Lazare, M., Li, J., & Plummer, D. (2008). The CCCma third generation AGCM and its extension into the middle atmosphere. *Atmospheric Chemistry and Physics*, *8*(23), 7055–7074.

Seidel, D. J., Li, J., Mears, C., Moradi, I., Nash, J., Randel, W. J., et al. (2016). Stratospheric temperature changes during the satellite era. *Journal of Geophysical Research: Atmospheres*, *121*, 664–681. https://doi.org/10.1002/2015JD024039

Shepherd, T. G., & McLandress, C. (2011). A robust mechanism for strengthening of the Brewer–Dobson circulation in response to climate change: Critical-layer control of subtropical wave breaking. *Journal of the Atmospheric Sciences*, *68*(4), 784–797.

Solomon, S., Kinnison, D., Bandoro, J., & Garcia, R. (2015). Simulation of polar ozone depletion: An update. *Journal of Geophysical Research: Atmospheres*, *120*, 7958–7974. https://doi.org/10.1002/2015JD023365

Taylor, K. E., Stouffer, R. J., & Meehl, G. A. (2012). An overview of CMIP5 and the experiment design. *Bulletin of the American Meteorological Society*, *93*(4), 485–498.

Velders, G. J. M., Andersen, S. O., Daniel, J. S., Fahey, D. W., & McFarland, M. (2007). The importance of the Montreal protocol in protecting climate. *Proceedings of the National Academy of Sciences of the United States of America*, *104*, 4814–1819.

World Meteorological Organization (2011). Scientific assessment of ozone depletion: 2010 (Global Ozone Research and Monitoring Project-Report No. 52). Geneva, Switzerland.

WMO (2014). Scientific assessment of ozone depletion: 2014 (Global Ozone Research and Monitoring Project-Report No. 55). Geneva, Switzerland.